Biophysical Chemistry 153 (2010) 17–26

Contents lists available at ScienceDirect

Biophysical Chemistry

journal homepage: http://www.elsevier.com/locate/biophyschem

Hierarchy of local structural and dynamics perturbations due to subdenaturing urea in the native state ensemble of DLC8 dimer

P.M. Krishna Mohan [1,2], Swagata Chakraborty [1], Ramakrishna V. Hosur *

Department of Chemical Sciences, Tata Institute of Fundamental Research, Homi Bhabha Road, Mumbai 400 005, India

ARTICLE INFO

Article history:
Received 27 July 2010
Received in revised form 28 September 2010
Accepted 29 September 2010
Available online 27 October 2010

Keywords:
Dynein Light Chain protein (DLC8)
Nuclear magnetic resonance
Equilibrium states
Unfolding mechanism
Circular dichroism
Fluorescence spectroscopy

ABSTRACT

Local structural and dynamic modulations due to small environmental perturbations reflect the adaptability of the protein to different interactors. We have investigated here the preferential local perturbations in Dynein light chain protein (DLC8), a cargo adapter, by sub-denaturing urea concentrations. Equilibrium unfolding experiments by optical spectroscopic methods indicated a two state like unfolding of DLC8 dimer, with the transition mid-point occurring around 8.6 M urea. NMR studies identified the β3 and β4 strands, N-, C- terminal regions, loops connecting β1 to α1, α1 to α2 and β3 to β4 as the soft targets of urea perturbation and thus indicated potential unfolding initiation sites. Native-state hydrogen exchange studies suggested the unfolding to traverse from the edges towards the centre of the secondary structural elements. At 6 M urea the whole protein chain acts like a cooperative unit. These observations are expected to have important implications for the protein's multiple functions.

1. Introduction

DLC8, the smallest (10.3 kDa, 89 residues) light chain of the dynein motor complex is a highly conserved protein that is found in all organisms [1,2]. DLC8 interacts with proteins of diverse biological functions [3–8]. The conserved nature, ubiquitous expression, multiple biochemical forms, and numerous cellular targets of DLC8 strongly suggest that the protein might be playing a conserved cellular function in multiple protein complexes [1,2,9] . DLC8 exists as a homo dimer at physiological pH and a monomer at pH 3 [10,11]. However, DLC8 is functional only in its dimeric form. The DLC8 dimer consists of two α-helices (α1, residues 15–31; α2, residues 35–50) and 5 β-strands (β1, residues 6–11; β2, residues 54–59; β3, residues 62–67; β4, residues 72–78 and β5, residues 81–87) [2]. DLC8 is involved in cargo trafficking across the cell. In this process it encompasses small folding/unfolding events accompanied with small structural/dynamic fluctuations in order to facilitate loading/unloading of cargo molecules. pH dependent native energy landscape analysis and target binding studies on DLC8 suggested small environmental perturbations can efficiently modulate target binding efficacies by regulating the dynamics of the dimer [12,13]. In view of this it is important to monitor the structural and motional behavior of the DLC8 in presence of various agents that cause differential local perturbations in the protein. These slight perturbations create ensemble of protein conformations which inter-convert amongst themselves and are important from the functional point of view of the protein.

Stability and unfolding features of DLC8 protein both in its dimeric and monomeric forms have been studied extensively using denaturants, guanidine hydrochloride and urea [10,14–19]. These denaturants interact differently with the folded protein; guanidine being positively charged leads to efficient hydrophobic collapse via electrostatic screening while urea is neutral and is a milder structure perturbing agent. Being a chaotropic agent, urea has been thought to disrupt hydrophobic interactions responsible for the globular structure of proteins [20–24]. However, recent studies on urea interaction with amino acids indicated that urea has preference for a favorable interaction at polar amide surface, located mostly on the peptide backbone [25,26]. Moreover, transfer model analysis by Auton et al. [27] clearly showed that urea's favorable interaction with peptide backbone is the driving force for urea-induced denaturation, with nonpolar group-urea interactions playing little or no role in the process. All these results strongly suggest that hydrogen bonds between urea and the protein backbone, contribute significantly to the overall energetics of urea denaturation [25–27].

There are numerous effects of urea that can influence protein function, such as solute-induced attenuation of hydrophobic/electrostatic interactions which are important between substrate and protein

Abbreviations: HSQC, Hetero nuclear single quantum coherence; TOCSY, Total correlation spectroscopy; HX, Hydrogen exchange; NHX, Native state hydrogen exchange; NOE, Nuclear overhauser effect; CPMG, Carr Purcell Meiboom Gill; TALOS, Torsion angle likelihood obtained from shift and sequence similarity; CD, Circular dichroism; GdnHCl, Guanidine Hydrochloride; aa, amino acids; DTT, Dithiothreitol.

* Corresponding author. Tel.: +91 22 2278 2488; fax: +91 22 2280 4610.
E-mail address: hosur@tifr.res.in (R.V. Hosur).

[1] Both authors contributed equally to this work.

[2] Present address: Department of Chemistry and Chemical Biology, Rutgers University, 610 Taylor Road, Piscataway, NJ, 08854, USA.

0301-4622/$ – see front matter © 2010 Elsevier B.V. All rights reserved.
doi:10.1016/j.bpc.2010.09.010

[28]. Moreover urea is present in the renal cells of many organisms. Thus, in view of the possible implications of urea interactions to protein stability and function, we explored here the preferential local perturbations by sub-denaturing urea concentrations in native DLC8. These, in some sense, also provide a simplistic identification of the initiation sites of DLC8 unfolding.

2. Materials and methods

2.1. Protein expression and purification

DLC8 was expressed and purified as described elsewhere [11,13].

2.2. Optical spectroscopy

2.2.1. Circular dichroism and fluorescence spectroscopy

Far-UV CD spectra were recorded at pH 7 on a JASCO model J-810 spectropolarimeter using a 1 nm bandwidth at 27 °C. The global unfolding of protein was monitored at 222 nm. Steady-state fluorescence emission spectra were recorded with $\lambda_{ex} = 295$ nm on a Spex Fluorolog-dM3000F spectrofluorimeter using a 1 cm path-length cuvette with a band pass of 1.5 nm for both excitation and emission. For all the experiments the protein concentration is 20 μM as a dimer (20 mM Tris, 200 mM NaCl, 2 mM DTT, pH 7). Denaturation profiles of DLC8 were measured as described by Chatterjee et al. [14] at 27 °C (also see Supplementary material).

2.2.2. Data analysis

The analysis of optical unfolding data of DLC8 is complicated because DLC8 is a dimer. Often the intermediate is not clearly identified by the optical techniques and the model D⟺2U, described as a two-state process can be used, with a concentration dependent second order dissociation/unfolding approximation.

The spectroscopic signal measured from the CD/fluorescence has been used to calculate fraction unfolded (monomeric protein) using Eq. (1) and the equilibrium constant was determined using concentration dependent second order dissociation Eq. (2).

$$f_u = \frac{S_d - S_i}{S_d - S_u} \tag{1}$$

$$K = \frac{[U]^2}{[D]} = \frac{2Pf_u^2}{1-f_u} \tag{2}$$

Where f_u is the apparent fraction unfolded, S_d is the spectroscopic signal associated with the pure dimer, S_u is the signal of the unfolded, S_i is the signal at varying concentrations of the denaturant, K is the equilibrium constant for unfolding, and P is the protein concentration.

The free energies at various concentrations of urea (ΔG_i) have been calculated using Eq. (3) and the free energy ΔG_i is calculated as $\Delta G_i = -RT \ln K_i$, (K_i obtained from Eq. (2)).

$$\Delta G_i = \Delta G - m[\text{Urea}] \tag{3}$$

The free energy change ΔG was determined by a fit for points in the transition region of the denaturation curve using a linear fitting. In the Eq. (3), ΔG is the intercept of the line which provides the free energy of denaturation or unfolding at 0 M urea and m is the slope of the line given by a plot of ΔG_i vs [Urea] [29–34].

2.3. NMR spectroscopy

2.3.1. NMR data acquisition, processing and analysis

For NMR studies the protein purified as described above was concentrated to ~1.0–1.5 mM. Tris buffer (20 mM Tris, 200 mM NaCl, 2 mM DTT, pH 7.0) was used for all the experiments. All NMR experiments were performed at 27 °C either on Bruker Avance 800 MHz or on Varian Unity-plus 600 MHz NMR spectrometer. ^{1}H chemical shifts were calibrated relative to 2,2-dimethyl-2-silapentane-5-sulfonate (DSS). All the triple resonance experiments required were recorded as discussed earlier [13,14]. Native state hydrogen exchange experiments (NHX) were carried out under the sub-denaturing conditions at various urea concentrations (2, 4 and 6 M) as discussed by Mohan et al. [18] Transverse relaxation rates (R_2) were measured with the following CPMG delays: 10, 30, 50, 70, 90, 110, 130, 150, 170 and 190 ms. Longitudinal relaxation rates (R_1) were measured with the following inversion recovery delays: 10, 50, 120, 220, 350, 500, 700 and 900 ms. For steady state heteronuclear (^{1}H–^{15}N) NOE experiments proton saturation time of 2.5 s and relaxation delay of 2.5 s were used. A relaxation delay of 2.5 s was used in the experiment without proton saturation.

All the data were processed using FELIX 2002. Residue specific cumulative chemical shift changes (ΔCS) at native state (0 M urea) and at different concentrations of urea (1 M, 2 M, 4 M and 6 M) were calculated as described earlier [16]. The most probable (ϕ,ψ) values were obtained from H^{α}, C^{α}, C^{β}, CO and ^{15}N chemical shifts by using the TALOS algorithm [35] for the urea perturbed states (2 M and 4 M Urea) as well for the native protein (0 M urea) for the purpose of comparison as described by Chatterjee et al. [14] and are listed in S1-Table (Supplementary material). The TALOS output file also provides the range of phi and psi deviations (δphi and δpsi). In order to calculate the significance of Δ (ϕ,ψ) values between two states we defined two new parameters given by

$$S_{phi} = |\Delta\phi| \sqrt{(k_{1,phi}^2 + k_{2,phi}^2)} \tag{4}$$

$$S_{psi} = |\Delta\psi| \sqrt{(k_{1,psi}^2 + k_{2,psi}^2)} \tag{5}$$

where, $k_{1,\text{phi}}$ and $k_{2,\text{phi}}$ are the ratios $\delta(\text{phi}_1)/\text{phi}_1$ and $\delta(\text{phi}_2)/\text{phi}_2$; $k_{1,\text{psi}}$ and $k_{2,\text{psi}}$ are the ratios $\delta(\text{psi}_1)/\text{psi}_1$ and $\delta(\text{psi}_2)/\text{psi}_2$ respectively and the suffices 1 and 2 indicate two different urea concentrations.

The R_1 and R_2 values were extracted by fitting the peak intensities to the equation, $I(t) = B \exp(-R_{1,2}t)$. Steady state ^{1}H–^{15}N NOE was calculated as a ratio of intensities of the peaks with and without proton saturation. The errors in the NOEs were obtained as described by Farrow et al. [36]. Reduced spectral density analysis was carried out for calculation of spectral densities as described by Chatterjee et al. [14]. For hydrogen exchange studies a series of HSQC spectra were recorded at regular intervals of time for around 12 h. These decays were fitted to single exponential functions to obtain the first order rate constants, k_{obs} and hence the protection factors as described elsewhere [18]. The highly protected non decaying residues are given a constant value of log (PF) = 9. The initial HSQC spectrum was recorded 8 min (dead time) after adding D_2O (S1-Figure, Supplementary material).

2.3.2. Resonance assignment of urea dependent HSQC spectra

The backbone resonance assignment of the DLC8 dimer (0 M urea) at pH 7, 27 °C was reported earlier [11,13]. We assigned the resonances in the HSQC spectra up to 6 M urea, in order to throw light on the urea induced perturbations to the protein. As the spectra were almost similar we were able to assign most of the resonances using direct transfer from the 0 M spectrum. However, in case of ambiguities, the resonances were confirmed with experiments such as CBCA(CO)NH and CBCANH. The number of peaks assigned in the HSQC spectra at 2 M, 4 M and 6 M urea are 88, 85 and 77 respectively.

3. Results and discussion

3.1. Urea induced equilibrium unfolding of DLC8 dimer

Equilibrium denaturation experiments using circular dichroism and steady state fluorescence provide a convenient way to understand

the protein folding/unfolding behavior. We investigated the stability and unfolding characteristics of DLC8 dimer using urea induced unfolding. Fig. 1(A–D) shows the raw data and the denaturation profiles of DLC8 dimer at pH 7, at different urea concentrations as obtained by means of far-UV CD spectroscopy and by fluorescence spectroscopy (Trp 54 fluorescence).

The curves obtained from CD and fluorescence fit to a two-state unfolding approximation (Fig. 1C, D). As DLC8 exists as a dimer under the chosen experimental conditions, the denaturation curves have been analyzed using the two-state model (best suited) $D \leftrightarrow 2U$ (discussed in Materials and methods), and the summary of the extracted thermodynamic parameters are given in Table 1. The transition mid points (Cm) obtained from two-state fits for CD (8.7 M) and steady-state fluorescence (8.6 M) profiles are similar hinting that the equilibrium unfolding of DLC8 appears to be a simple two-state process. However, we observed that the thermodynamic parameters (m-values and ΔG) obtained from CD and fluorescence (Table 1) are different to a certain extent. Moreover, the spectral profiles of CD and fluorescence above 6 M urea are also different (Fig. 1A, B). Both these facts suggest that the denaturation of DLC8 dimer is more complex. Further, Fig. 1A reveals that the DLC8 dimer retains its native secondary folds until 7 M urea whereas, the transition in the tertiary structure sets in from 6 M urea as revealed from the fluorescence curves (Fig. 1B). As DLC8 dimer remains in native state up to 6 M urea, the NMR characterization of the equilibrium states of DLC8 until 6 M urea will provide snapshots of the early unfolding interactions at a residue level.

Table 1
Summary of the thermodynamic parameters for urea denaturation of DLC8, at pH 7.0.

	Model	m (kcal mol^{-1} M^{-1})	ΔG (kcal mol^{-1})	C_m (M)
Fluorescence	$D \Leftrightarrow 2U$	1.64 ± 0.05	14 ± 0.3	8.6
CD	$D \Leftrightarrow 2U$	1.89 ± 0.04	16.4 ± 0.5	8.7

3.2. NMR characterization of the urea perturbed equilibrium states

Considering the structural and motional perturbations created by sub-denaturing conditions of urea are highly relevant to understand the structural adaptability and the initial unfolding events, we investigated the equilibrium states of DLC8 dimer created by different urea concentrations (0 M to 6 M) at residue level using a variety of NMR probes. These NMR probes reveal the small local perturbations that might occur due to the vulnerability of that particular site of the protein to the denaturant thereby leading to specific interactions of the protein chain which otherwise are not detectable through normal optical spectroscopic studies.

^{1}H–^{15}N HSQC spectrum is the fingerprint of a protein conformation. Fig. 2A shows the HSQC spectra of DLC8 at various concentrations of urea (0 M to 10 M). The HSQC spectra from 0 M to 4 M urea are largely similar suggesting that the protein exists as a dimeric species under these experimental conditions. The 6 M spectrum does however contains additional peaks which would imply some local unfolding. At 8 M urea (Fig. 2A), nearer to the transition melting point (~8.6 M urea,

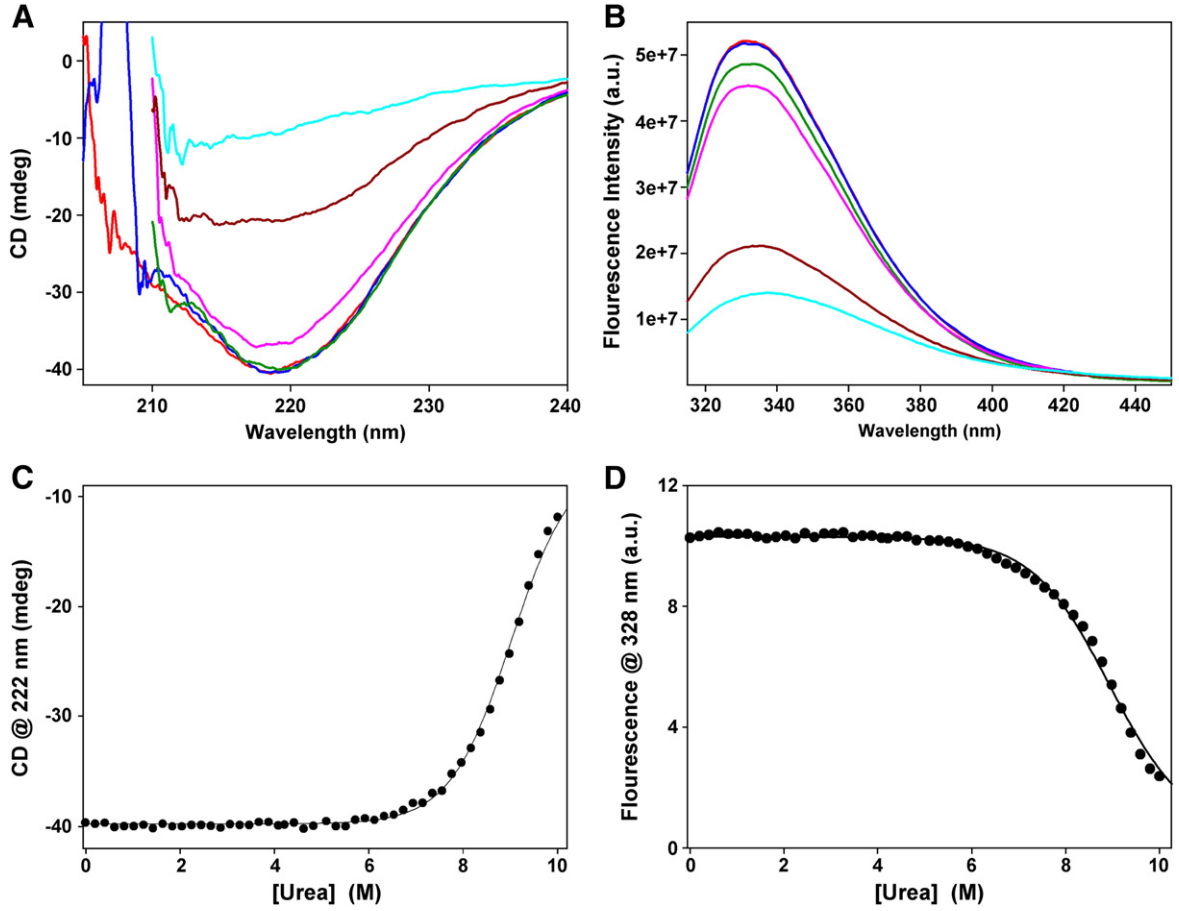

Fig. 1. Denaturation profile of DLC8. (A) Far-UV circular dichroism and (B) fluorescence spectra of DLC8 protein under different urea concentrations: Red (0 M), Blue (6 M), Green (7 M), Pink (8 M), Brown (9 M), Cyan (10 M). Spectroscopic parameters for the unfolding profile of DLC8 dimer obtained from (C) circular dichroism and (D) steady state fluorescence; are plotted against concentration of urea. The solid lines represent the best fits obtained as described in Materials and methods (Supplementary material).

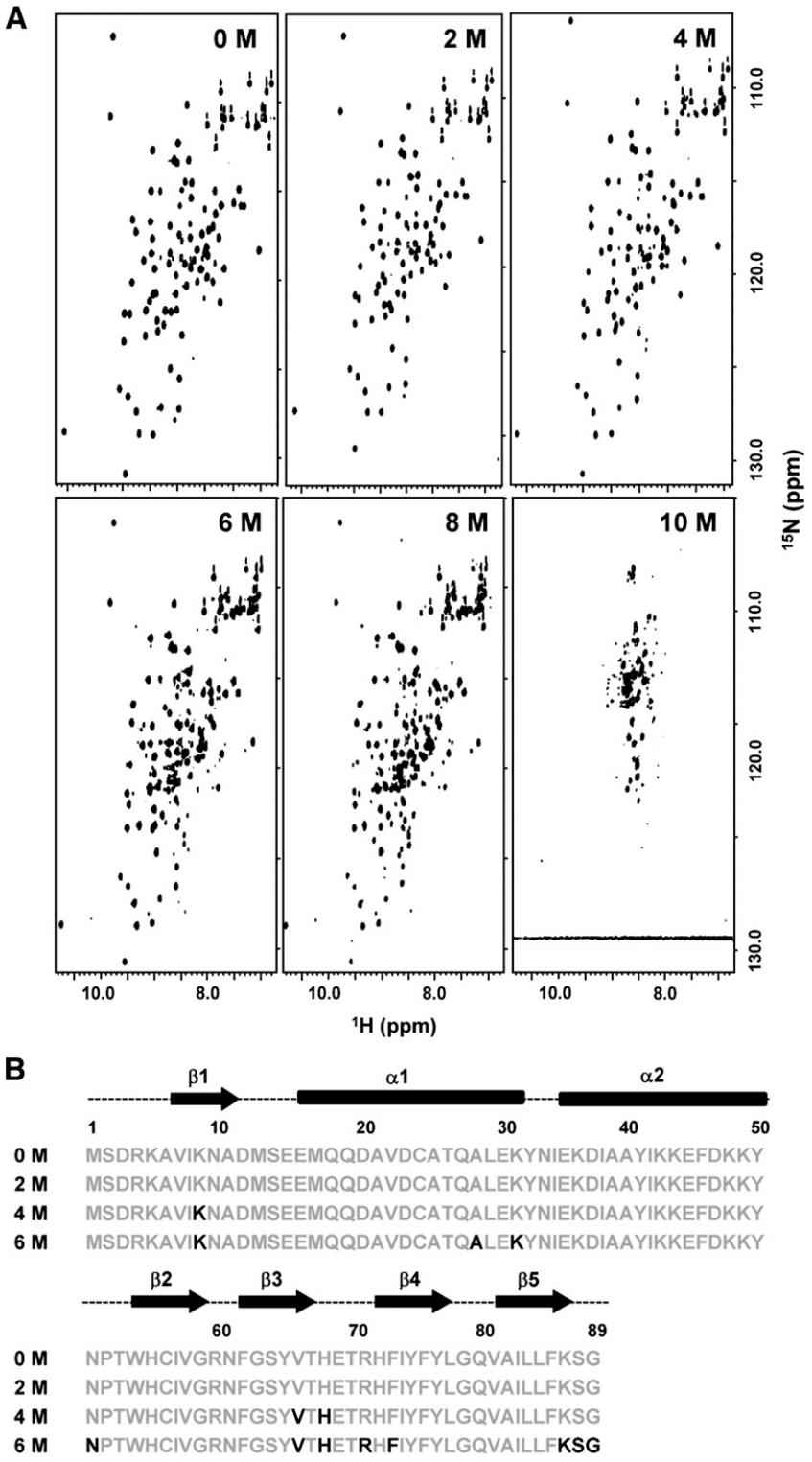

Fig. 2. ^{1}H–^{15}N HSQC spectra at various urea concentrations. (A) ^{1}H–^{15}N HSQC spectra of DLC8 protein at pH 7, 27 °C at various urea concentrations (0 M to 10 M) (B) Summary of the residues broadened during the sequential urea induced unfolding (0 M to 6 M) of DLC8 dimer: the broadened residues have been marked (black) on the primary sequence of the protein. The secondary structural elements in the protein are marked above with cylinders (for helices) and arrows (for sheets).

Table 1), the spectrum is a mixture of several species rather than a pure dimeric protein; the other species populating the spectra could be the partially collapsed dimer, and/or the monomeric protein and also the unfolded protein. Finally at 10 M urea (Fig. 2A), the spectrum correspond to the unfolded state, which is evident from the narrow dispersion of the peaks in both amide proton and nitrogen dimensions. We observed that at higher concentrations of urea (4 M and 6 M), some peaks disappeared due to large line broadening effects. The peaks that broadened due to such exchange are marked with black on the primary sequence of the protein (Fig. 2B).

3.2.1. Structural and dynamic perturbations

Amide proton and ^{15}N chemical shifts are sensitive probes for the local environment of a given residue in a protein structure. H^{α}, $^{13}C^{\alpha}$,

and $^{13}C'$ chemical shifts of an amino acid residue in a folded protein have a well-established correlation with secondary structures [37–40] and hence the most probable dihedral angles (ϕ,ψ). We calculated the amide proton chemical shift perturbations [16] and (ϕ,ψ) values from H^{α}, C^{α}, C^{β}, CO and ^{15}N chemical shifts by using the TALOS algorithm [35] as described in Materials and methods. The results of these calculations are shown in Figs. 3 and 4. The local structural perturbations (Fig. 3) vary significantly along the sequence above 1 M urea. At 2 M urea, the local perturbations are initiated at the β3 and β4 strands, N-, C- terminal regions, loops connecting α1 to α2 and β3 to β4. The perturbations in the region of β3 and β4 strands and its interconnecting loop, which is a part of the dimer interface and also the cargo binding site of the protein may have direct functional relevance. It has been reported that this segment of the dimeric protein is the most vulnerable region for external perturbations [17]. At 4 M urea, the local structural perturbations extend along the helical segments (α1, α2).

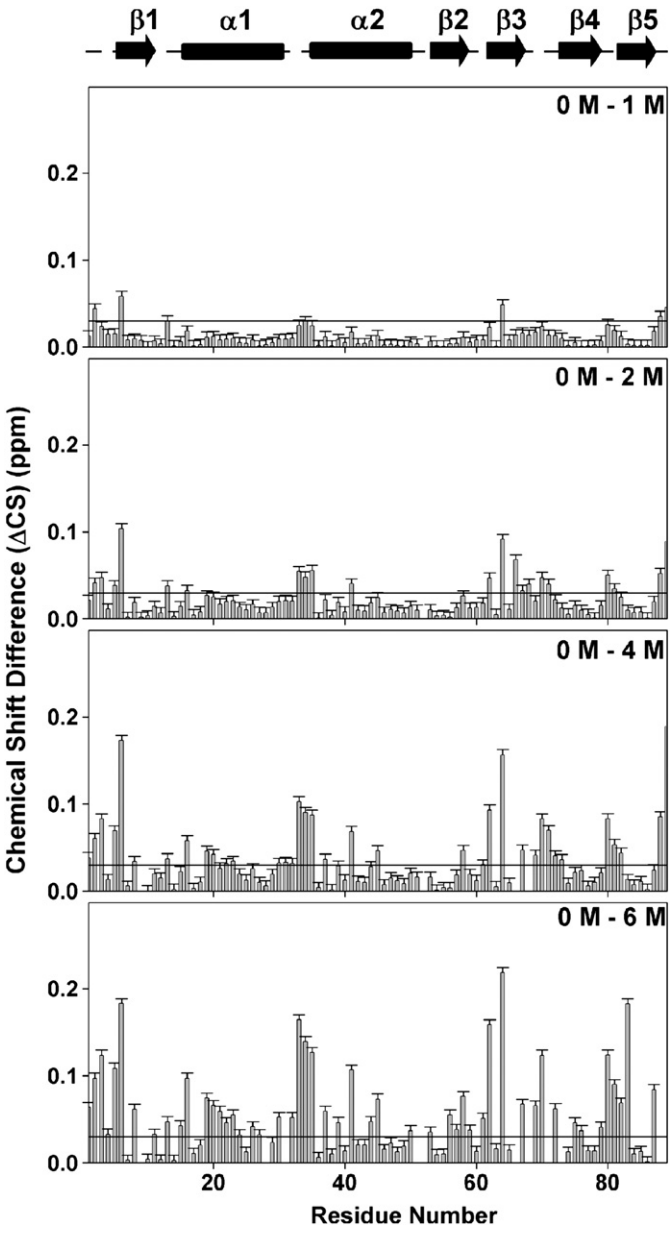

Fig. 3. Chemical shift perturbation. Residue specific summed chemical shift changes ($\Delta\delta$) calculated from ΔH^N and ΔN shifts for DLC8 protein between 0 M urea and at different urea concentrations 1 M, 2 M, 4 M and 6 M. The horizontal line indicates the cut-off of the deviations. This corresponds to more than twice the maximum error in the individual chemical shift measurements.

From the difference in (ϕ,ψ) values up to 4 M urea (between 0–2 M urea and 0–4 M urea) (Fig. 4), it is evident that there are certain regions in the protein, that are conspicuously perturbed due to the specific interactions with the denaturant. These regions show up in both ϕ, ψ values, although some of them are more pronounced in the ψ values. The perturbed segments are mainly concentrated in the interconnecting loops and/or at the edges of the structural elements (Fig. 4). The most perturbed regions are loops connecting β1 to α1, α1 to α2 and β2 to β3, the C-terminal edge of α2 and the N-terminal of β3 sheet. However, the overall deviations in the torsion angles over the polypeptide chain are small, suggesting that there is no drastic change in the secondary structure of the protein under these conditions (up to 4 M urea).

As the structural perturbations are accompanied with variations in the motional characteristics and the conformational dynamics of the protein molecule, we carried out ^{15}N relaxation measurements on the protein in the folded state as well as at various urea concentrations. Residue specific transverse relaxation rates (R_2) reveal some distinct patterns (Fig. 5). In the native state large R_2 values in the region spanning residues 65 to 74, belonging to the loop between β3 and β4, and partly to β3 and β4 sheets suggest high degree of slow conformational transitions in this segment of the molecule [11,41]. It is evident from Fig. 5 that qualitatively the patterns of the R_2 values are almost conserved up to 4 M urea.

Finally at 6 M urea, we observe noticeable changes in the chemical shifts (Fig. 3) across the whole polypeptide chain, suggesting that structural perturbations encompass all the structural elements and their interconnecting loops. This indicates towards enhanced conformational/structural fluctuations in all segments. This is also evident from the 6 M HSQC spectrum (Fig. 2A) of the protein, where we saw several other resonances corresponding to various minor conformations appearing, although the dimeric species in the native state is still the predominant conformation. However, at 6 M urea, several residues disappear due to line broadening effects (Fig. 2B). Further, the residues in the β3 to β4 loop (aa. 65 –74), have almost similar R_2 values as the remaining polypeptide chain suggesting uniform motional preferences in this state of the dimeric protein. However, no noticeable changes were observed in the high frequency picosecond time scale motions as obtained from ^1H–^{15}N steady state NOEs (S2-Figure), indicating no major dynamic changes occurring at the faster timescales in the protein backbone under the chosen experimental conditions.

Further insights into the motional characteristics were obtained from the spectral density functions $J(0)$, $J(\omega_N)$ and $J(\omega_H)$ that provided direct information on both the slow (milli- to micro second time scale) and fast (nano second and pico second) time scale motions in the protein [42–44] in the native state and the urea perturbed states (S3-Figure). Interestingly, there is a fair degree of variation in the spectral densities, J(0) and $J(\omega_N)$. The high frequency spectral density, $J(\omega_H)$, is rather uniform across the polypeptide chain, both in the presence and absence of urea. This suggests that until 6 M urea perturbations the protein lacks any additional high frequency motions compared to the native state, which is completely in line with the conclusions drawn from ^1H–^{15}N steady state NOEs.

3.2.2. Stability of the DLC8 dimer and hierarchy of local perturbations under sub-denaturing conditions

To understand the structural stability and hierarchy of the urea induced perturbations in the DLC8 dimer, native state hydrogen exchange experiments have been performed. The protection factors calculated at all urea concentrations are given in Fig. 6. It is worth noting that the structural elements of DLC8 dimer have differential stability in its native state [18,19]. Fig. 7 represents the summary of protection factors marked with gradient coloring on the three dimensional structure of the protein (PDB ID: 1f3c). It is important to note here that with the increase in urea concentration there is a

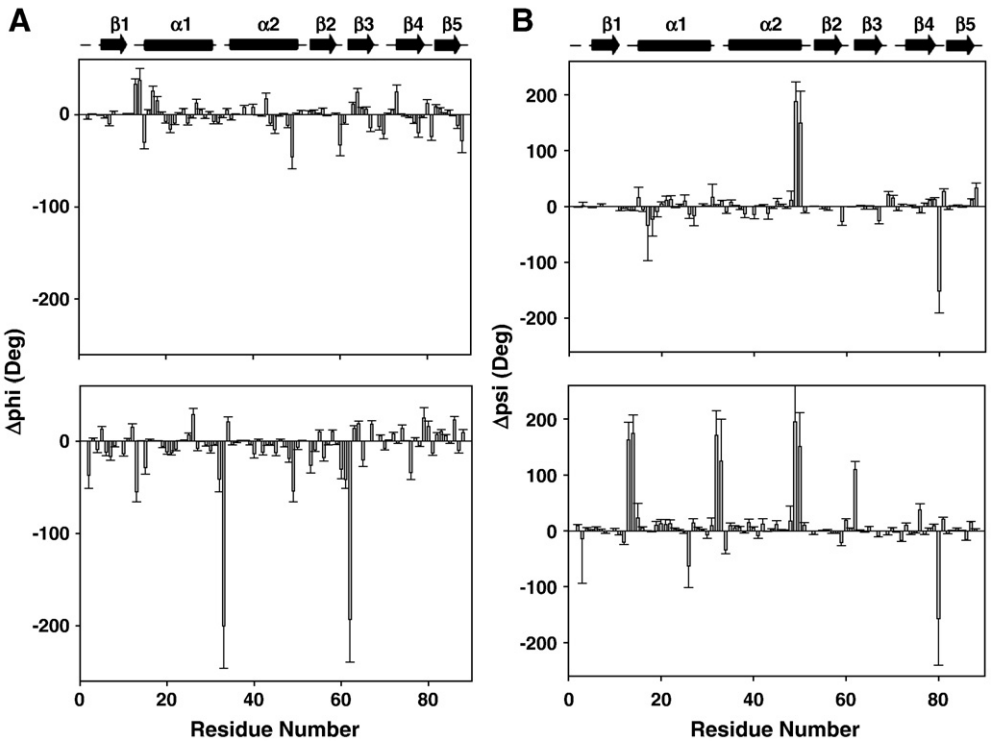

Fig. 4. Torsion angle perturbation. Residue specific changes in (ϕ, ψ) values for DLC8 protein at different urea concentrations were calculated using the TALOS algorithm [35]. The plots (A) Δphi and (B) Δpsi, show deviations with increasing urea concentrations as: 0 M–2 M (top panel) and 0 M–4 M (bottom panels). The error bars in the figure indicate the significance of deviations of phi and psi for each residue as described in material and methods.

decrease in the extent of protection and the loss of protection traverses from the edge towards the centre of the structural elements, this may reflect the "hierarchy" of local perturbations. It is evident from Figs. 6 & 7 that the dimeric protein has differential segmental stability in its native state and also in the presence of urea up to 4 M. However, at 6 M urea, all the segments have almost similar stability suggesting that the molecule is acting as a single co-operative unit. This is also in accordance with the motional characteristics and chemical shift perturbations discussed above.

3.3. DLC8 dimer unfolds via a monomer

In order to obtain more insights into the complex nature of unfolding transition and the variety of the species present at the transition zone of the denaturation curve in urea, we recorded the NMR spectrum of the DLC8 dimer at 8 M urea (Figs. 2A & 8). It is evident from the spectrum that the number of peaks present in the spectrum is much more compared to the dimeric species (88 backbone resonances). We compared the HSQC spectrum at 8 M urea with those of the dimeric species, the denatured protein (Fig. 2A) and the monomeric DLC8 (H55K) mutant at pH 7 (Fig. 8). A few peaks corresponding to the monomer are identified and marked in Fig. 8 for illustration. From Figs. 2A and 8 it is reasonable to conclude that, during the unfolding transition, DLC8 monomer is present.

3.4. Comparison of the initial events in the denaturation process induced by urea with those by guanidine–hydrochloride

Guanidine–HCl and urea are completely different genres of denaturants and their denaturation mechanisms also vary. Thus one expects important differences in their effects on the protein structure and dynamics. In view of these, the comparative study of the response of the DLC8 protein to differential external perturbations by urea and Gdn–HCl is significant. Though certain similar behaviors were observed in the various segments of the dimeric protein under the influence of both the denaturants, there are certain differences also.

The first point of difference lies in the signature of unfolding curve in the two cases as monitored by CD and fluorescence (Fig. 9). In the case of urea, both CD and fluorescence yield similar denaturation profiles indicating towards a two state transition. In the presence of Gdn–HCl, however, the curves obtained from CD and fluorescence do not superimpose suggesting that the equilibrium unfolding of the protein is complex with accumulation of stable intermediates [10,17]. This indicates that the nature of the intermediates accumulated in the initial stages of unfolding transition induced by urea and Gdn–HCl are different. Indeed, similar differences have been previously reported for the monomer [14]. However, in the present case we cannot rule out the possibility of the insensitivity of these optical probes to sense the structural changes of the protein during the denaturation process especially when the intermediate species are sparsely populated and have very high structural similarity (as like DLC8 dimer and monomer) to that of the native protein.

DLC8 dimer remains in its native state ensemble (Fig. 2) until 4 M urea. However the spectrum at 6 M urea shows some additional resonances resulting from the onset of unfolding transitions. This is consistent with the fluorescence curve (Fig. 1B). At 6 M urea the residues disappearing due to line broadening effects (Fig. 2B) are concentrated mainly in the C-terminal end and the loop between β3 and β4 sheet. These segments of the protein may thus be assumed to be the most vulnerable sites for urea perturbation. In contrast, in presence of Gdn–HCl the conformational transitions are conspicuous in the N-terminal end, the loop between β2 and β3 sheets, the loop between β3 and β4 sheets and the C-terminal end. This indicates that the extent of perturbation is comparatively more widespread in case of Gdn–HCl. Secondly, at 6 M urea, the entire polypeptide chain has almost similar R_2 values suggesting uniform motional preferences in

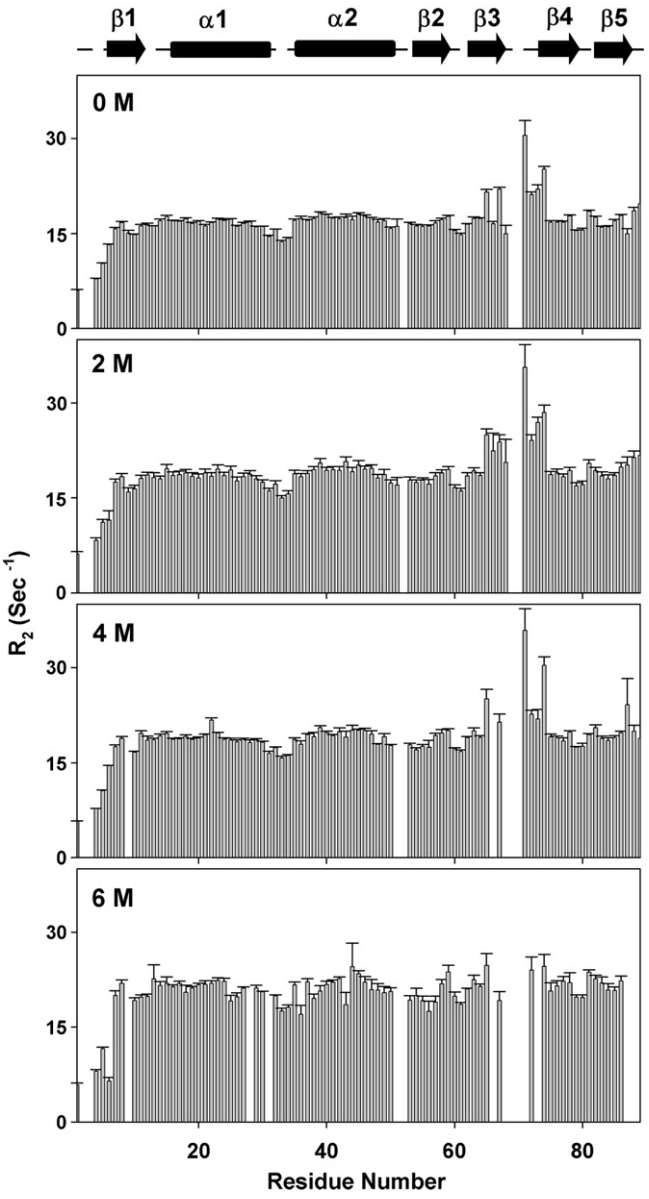

Fig. 5. Transverse relaxation rates. Residue specific ^{15}N transverse relaxation rates (R_2) for DLC8 protein at different urea concentrations: 0 M, 2 M, 4 M and 6 M.

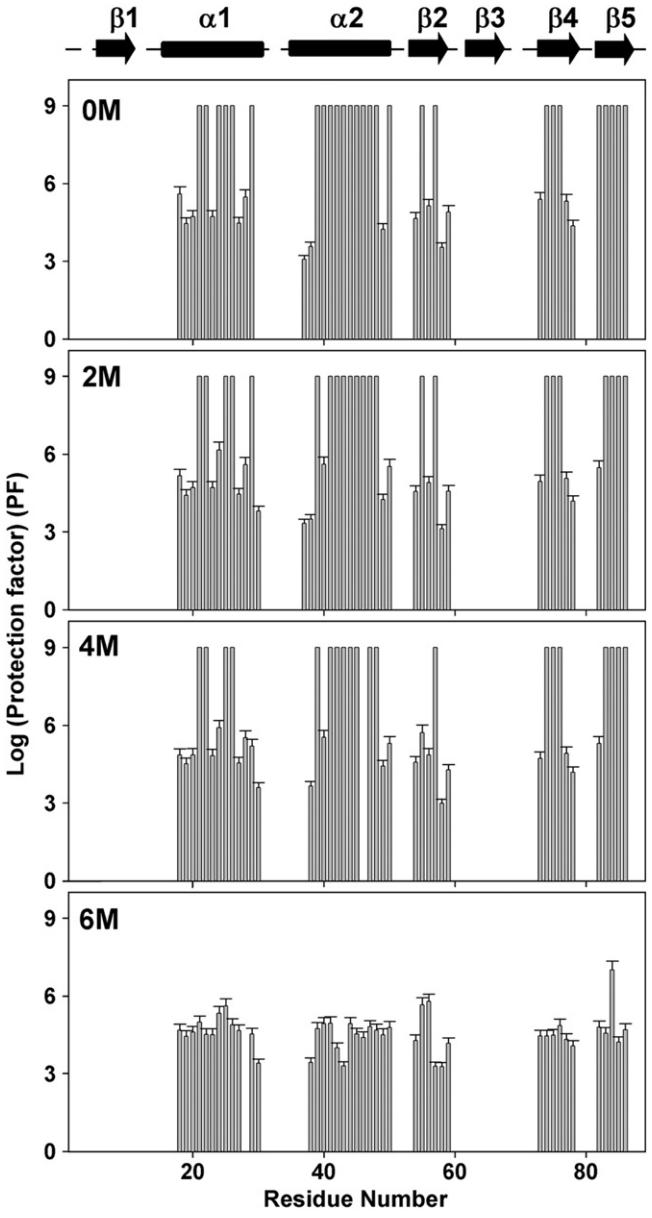

Fig. 6. Protection factors (PFs) from hydrogen exchange. Residue specific protection factors (PFs) for DLC8 protein at different urea concentrations, 0 M, 2 M, 4 M and 6 M. A protection factor (PF) of 9 is given to the residues that are not decayed during the measurement time (12 h, see Materials and methods).

this state of the dimeric protein (Fig. 5). Such is not the case of the protein in presence of Gdn–HCl in the pre transition zone. Hence, it can be assumed that the unfolding transition is more cooperative in urea than in guanidine–hydrochloride.

4. Conclusion

Our NMR approaches have revealed several interesting facts related to the structural and dynamic behavior of the DLC8 dimer to urea perturbation in the pre transition zone at a residue level. The denaturation curves derived from optical spectroscopic data revealed a two-state transition like profile unlike in the case of guanidine–hydrochloride. However, intricate detailing revealed more complex process with accumulation of sparsely populated intermediates. Various NMR probes were used to identify the initial structural and motional perturbations of the protein in the presence of urea. Until 4 M urea, the behavior of the protein was found to be quite similar to the native protein with slight local perturbations. These initial perturbation sites include the β3 and β4 strands, N-, C- terminal regions, loops connecting β1 to α1, α1 to α2 and β3 to β 4. These regions may act as potential unfolding initiation sites. The modulations in the cargo binding sites, i.e. β3 and β4 strands and their interconnecting loops in the presence of external perturbant reflect the adaptability of the protein's function in response to the solvent environment. Interestingly, at 6 M urea, the perturbations become more conspicuous. At this stage the secondary structural elements of the protein start loosening and the protein behaves more like a single unit with uniform motional preferences throughout the polypeptide chain. The HSQC spectrum at 8 M urea, close to the transition midpoint shows population of multiple conformations, one of those corresponds to the monomer. The stability and hierarchy of local perturbations in the dimer in presence of urea, probed by HX gave us a direct glimpse of the variable extent of vulnerability of the residues of the dimeric protein on urea perturbation. The α2 helix, the β4 and the β5 sheets were found to be initially more

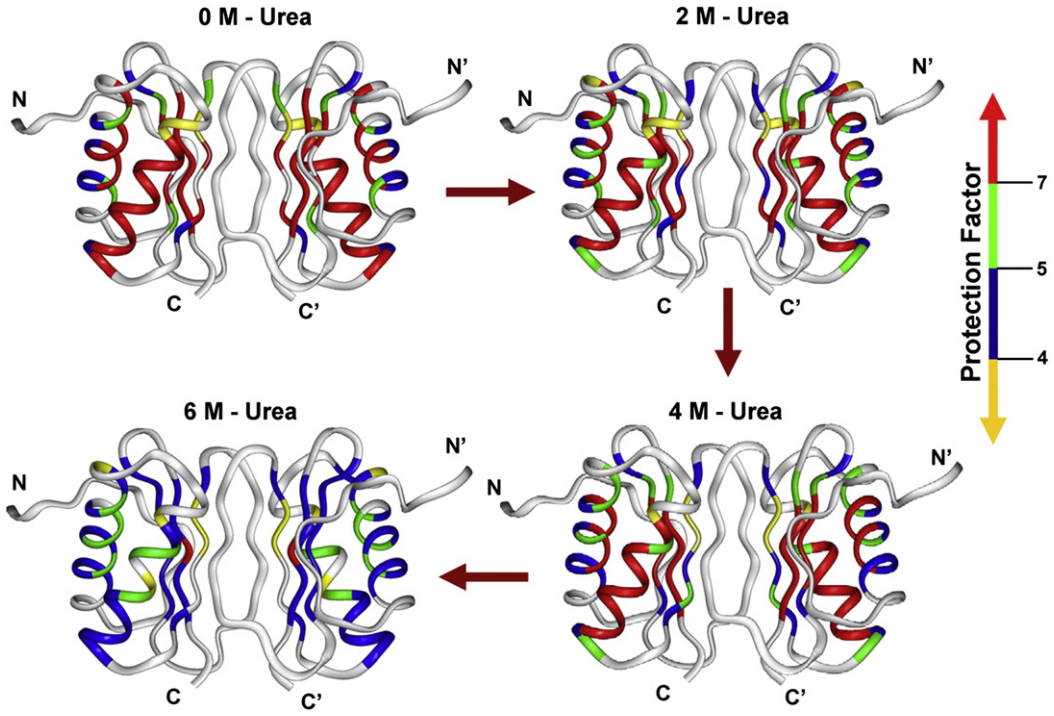

Fig. 7. Hierarchy of amide proton protection. Summary of protection factors marked with gradient coloring on the three dimensional structure of the protein (PDB ID: 1f3c). The color codes are: yellow<4, 4<blue<5, 5<green<7 and red>7. The residues which are not decayed during the measurement time (PF = 9) are given red color. The primed and the unprimed labels distinguish the two monomers. The images were produced using Insight II.

protected from urea perturbation than the other structural elements. With increasing urea concentration, the probable hierarchy of unfolding seemed to originate from the edge of the structural elements and gradually move towards the centre. Until 4 M urea, the differential stability pattern of the structural elements were more or less conserved as that in the native state, but the protein displayed uniform protection throughout the polypeptide chain at 6 M urea indicative of some sort of cooperative nature of the protein at the pre transition zone. All these facts point towards the possibility of a more concerted transition with simultaneous dissociation of the dimer into monomer and unfolding of

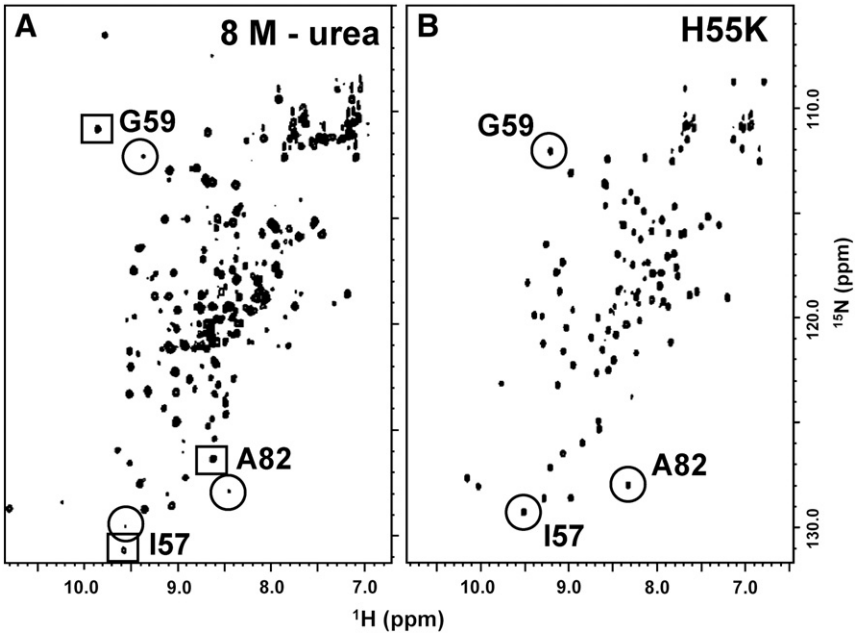

Fig. 8. Comparison with monomeric mutant H55K. $^{1}H^{N}$–^{15}N HSQC spectrum of DLC8 protein at pH 7, 27 °C with (A) 8 M urea (B) H55K mutant which is a monomer at pH 7, 27 °C. Residues I57, G59, A82 corresponding to the monomeric and dimeric species are annotated and marked with circles and squares respectively as illustrative examples.

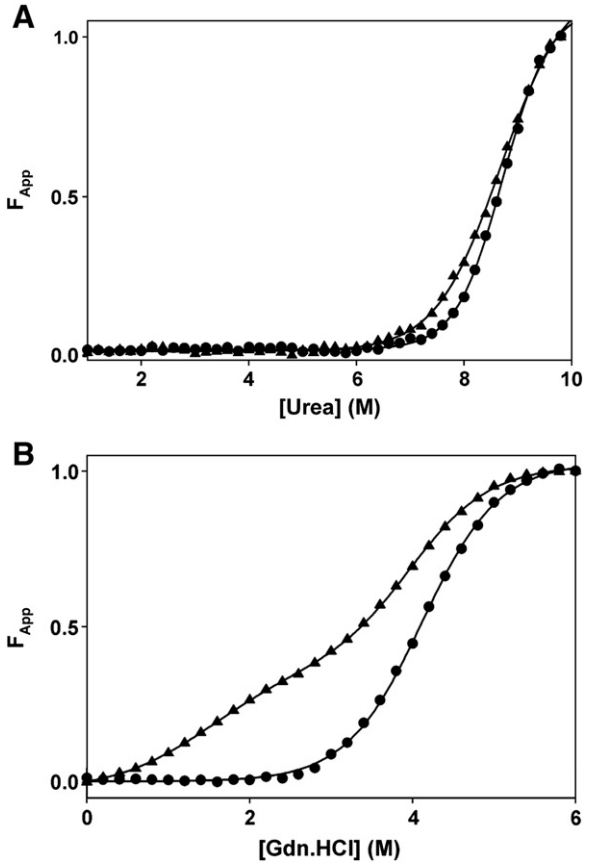

Fig. 9. Equilibrium unfolding profile of DLC8 by optical spectroscopy. Normalized spectroscopic parameters (fraction apparent – F_{app}) for the unfolding profile of DLC8 dimer obtained from circular dichroism (circles) and steady state fluorescence (triangles); are plotted against concentration of (A) Urea (B) Gdn–HCl. The solid lines represent the best fits obtained as described in Materials and methods (Supplementary material).

the monomer in presence of urea as denaturant. These features are distinctly different from those induced by Gdn–HCl perturbation that results in the accumulation of stable intermediates.

Acknowledgements

We thank the Government of India for providing financial support to the National Facility for High Field NMR at TIFR and Dr. Anindya Ghosh-Roy for the DLC8 clone.

Appendix A. Supplementary data

Supplementary data to this article can be found online at doi:10.1016/j.bpc.2010.09.010.

References

[1] S.M. King, E. Barbarese, J.F. Dillman III, R.S. Patel-King, J.H. Carson, K.K. Pfister, Brain cytoplasmic and flagellar outer arm dyneins share a highly conserved Mr 8, 000 light chain, J. Biol. Chem. 271 (1996) 19358–19366.
[2] J. Liang, S.R. Jaffrey, W. Guo, S.H. Snyder, J. Clardy, Structure of the PIN/LC8 dimer with a bound peptide, Nat. Struct. Biol. 6 (1999) 735–740.
[3] J.C. Fuhrmann, S. Kins, P. Rostaing, F.O. El, J. Kirsch, M. Sheng, A. Triller, H. Betz, M. Kneussel, Gephyrin interacts with Dynein light chains 1 and 2, components of motor protein complexes, J. Neurosci. 22 (2002) 5393–5402.
[4] S.R. Jaffrey, S.H. Snyder, PIN: an associated protein inhibitor of neuronal nitric oxide synthase, Science 274 (1996) 774–777.
[5] K.W. Lo, S. Naisbitt, J.S. Fan, M. Sheng, M. Zhang, The 8-kDa dynein light chain binds to its targets via a conserved (K/R)XTQT motif, J. Biol. Chem. 276 (2001) 14059–14066.
[6] H. Puthalakath, D.C. Huang, L.A. O'Reilly, S.M. King, A. Strasser, The proapoptotic activity of the Bcl-2 family member Bim is regulated by interaction with the dynein motor complex, Mol. Cell 3 (1999) 287–296.
[7] R.K. Vadlamudi, R. Bagheri-Yarmand, Z. Yang, S. Balasenthil, D. Nguyen, A.A. Sahin, H.P. den, R. Kumar, Dynein light chain 1, a p21-activated kinase 1-interacting substrate, promotes cancerous phenotypes, Cancer Cell 5 (2004) 575–585.
[8] Z. Yang, R.K. Vadlamudi, R. Kumar, Dynein light chain 1 phosphorylation controls macropinocytosis, J. Biol. Chem. 280 (2005) 654–659.
[9] S.M. King, R.S. Patel-King, The M(r) = 8,000 and 11,000 outer arm dynein light chains from Chlamydomonas flagella have cytoplasmic homologues, J. Biol. Chem. 270 (1995) 11445–11452.
[10] E. Barbar, B. Kleinman, D. Imhoff, M. Li, T.S. Hays, M. Hare, Dimerization and folding of LC8, a highly conserved light chain of cytoplasmic dynein, Biochemistry 40 (2001) 1596–1605.
[11] P.M. Mohan, M. Barve, A. Chatterjee, R.V. Hosur, pH driven conformational dynamics and dimer-to-monomer transition in DLC8, Protein Sci. 15 (2006) 335–342.
[12] P.M. Krishna Mohan, R.V. Hosur, NMR insights into dynamics regulated target binding of DLC8 dimer, Biochem. Biophys. Res. Commun. 355 (2007) 950–955.
[13] P.M. Krishna Mohan, M. Barve, A. Chatterjee, A. Ghosh-Roy, R.V. Hosur, NMR comparison of the native energy landscapes of DLC8 dimer and monomer, Biophys. Chem. 134 (2008) 10–19.
[14] A. Chatterjee, P.M. Krishna Mohan, A. Prabhu, A. Ghosh-Roy, R.V. Hosur, Equilibrium unfolding of DLC8 monomer by urea and guanidine hydrochloride: distinctive global and residue level features, Biochimie 89 (2007) 117–134.
[15] P.M. Krishna Mohan, Unfolding energetics and conformational stability of DLC8 monomer, Biochimie 89 (2007) 1409–1415.
[16] P.M. Mohan, R.V. Hosur, pH dependent unfolding characteristics of DLC8 dimer: residue level details from NMR, Biochim. Biophys. Acta 1784 (2008) 1795–1803.
[17] P.M. Mohan, M.V. Joshi, R.V. Hosur, Hierarchy in guanidine unfolding of DLC8 dimer: regulatory functional implications, Biochimie 91 (2009) 401–407.
[18] P.M. Mohan, S. Chakraborty, R.V. Hosur, Residue-wise conformational stability of DLC8 dimer from native-state hydrogen exchange, Proteins 75 (2009) 40–52.
[19] P.M. Mohan, S. Chakraborty, R.V. Hosur, NMR investigations on residue level unfolding thermodynamics in DLC8 dimer by temperature dependent native state hydrogen exchange, J. Biomol. NMR 44 (2009) 1–11.
[20] T.E. Creighton, Characterizing intermediates in protein folding, Curr. Biol. 1 (1991) 8–10.
[21] J.W. Wu, Z.X. Wang, New evidence for the denaturant binding model, Protein Sci. 8 (1999) 2090–2097.
[22] Q. Zou, S.M. Habermann-Rottinghaus, K.P. Murphy, Urea effects on protein stability: hydrogen bonding and the hydrophobic effect, Proteins 31 (1998) 107–115.
[23] Y. Nozaki, C. Tanford, The solubility of amino acids and related compounds in aqueous urea solutions, J. Biol. Chem. 238 (1963) 4074–4081.
[24] P.H. Yancey, G.N. Somero, Counteraction of urea destabilization of protein structure by methylamine osmoregulatory compounds of elasmobranch fishes, Biochem. J. 183 (1979) 317–323.
[25] M.C. Stumpe, H. Grubmuller, Interaction of urea with amino acids: implications for urea-induced protein denaturation, J. Am. Chem. Soc. 129 (2007) 16126–16131.
[26] J.G. Cannon, C.F. Anderson, M.T. Record Jr., Urea-amide preferential interactions in water: quantitative comparison of model compound data with biopolymer results using water accessible surface areas, J. Phys. Chem. B 111 (2007) 9675–9685.
[27] M. Auton, L.M. Holthauzen, D.W. Bolen, Anatomy of energetic changes accompanying urea-induced protein denaturation, Proc. Natl. Acad. Sci. U. S. A. 104 (2007) 15317–15322.
[28] D.W. Bolen, J.R. Fisher, Kinetic properties of adenosine deaminase in mixed aqueous solvents, Biochemistry 8 (1969) 4239–4246.
[29] D.W. Bolen, M.M. Santoro, Unfolding free energy changes determined by the linear extrapolation method. 2. Incorporation of delta G degrees N–U values in a thermodynamic cycle, Biochemistry 27 (1988) 8069–8074.
[30] J.U. Bowie, R.T. Sauer, Equilibrium dissociation and unfolding of the Arc repressor dimer, Biochemistry 28 (1989) 7139–7143.
[31] J.K. Grimsley, J.M. Scholtz, C.N. Pace, J.R. Wild, Organophosphorus hydrolase is a remarkably stable enzyme that unfolds through a homodimeric intermediate, Biochemistry 36 (1997) 14366–14374.
[32] K.E. Neet, D.E. Timm, Conformational stability of dimeric proteins: quantitative studies by equilibrium denaturation, Protein Sci. 3 (1994) 2167–2174.
[33] B.W. Noland, L.J. Dangott, T.O. Baldwin, Folding, stability, and physical properties of the alpha subunit of bacterial luciferase, Biochemistry 38 (1999) 16136–16145.
[34] M.M. Santoro, D.W. Bolen, Unfolding free energy changes determined by the linear extrapolation method. 1. Unfolding of phenylmethanesulfonyl alpha-chymotrypsin using different denaturants, Biochemistry 27 (1988) 8063–8068.
[35] G. Cornilescu, F. Delaglio, A. Bax, Protein backbone angle restraints from searching a database for chemical shift and sequence homology, J. Biomol. NMR 13 (1999) 289–302.
[36] N.A. Farrow, R. Muhandiram, A.U. Singer, S.M. Pascal, C.M. Kay, G. Gish, S.E. Shoelson, T. Pawson, J.D. Forman-Kay, L.E. Kay, Backbone dynamics of a free and phosphopeptide-complexed Src homology 2 domain studied by 15 N NMR relaxation, Biochemistry 33 (1994) 5984–6003.
[37] S. Schwarzinger, G.J. Kroon, T.R. Foss, P.E. Wright, H.J. Dyson, Random coil chemical shifts in acidic 8 M urea: implementation of random coil shift data in NMR View, J. Biomol. NMR 18 (2000) 43–48.
[38] S. Schwarzinger, G.J. Kroon, T.R. Foss, J. Chung, P.E. Wright, H.J. Dyson, Sequence-dependent correction of random coil NMR chemical shifts, J. Am. Chem. Soc. 123 (2001) 2970–2978.

[39] D.S. Wishart, B.D. Sykes, Chemical shifts as a tool for structure determination, Meth. Enzymol. 239 (1994) 363–392.
[40] D.S. Wishart, C.G. Bigam, A. Holm, R.S. Hodges, B.D. Sykes, 1 H, 13 C and 15 N random coil NMR chemical shifts of the common amino acids. I. Investigations of nearest-neighbor effects, J. Biomol. NMR 5 (1995) 67–81.
[41] J.S. Fan, Q. Zhang, H. Tochio, M. Zhang, Backbone dynamics of the 8 kDa dynein light chain dimer reveals molecular basis of the protein's functional diversity, J. Biomol. NMR 23 (2002) 103–114.
[42] J.F. Lefevre, K.T. Dayie, J.W. Peng, G. Wagner, Internal mobility in the partially folded DNA binding and dimerization domains of GAL4: NMR analysis of the N–H spectral density functions, Biochemistry 35 (1996) 2674–2686.
[43] J.W. Peng, G. Wagner, Mapping of the spectral densities of N–H bond motions in eglin c using heteronuclear relaxation experiments, Biochemistry 31 (1992) 8571–8586.
[44] P. Zhang, K.T. Dayie, G. Wagner, Unusual lack of internal mobility and fast overall tumbling in oxidized flavodoxin from *Anacystis nidulans*, J. Mol. Biol. 272 (1997) 443–455.